

RESEARCH

Open Access



# Dixon chemical shift MR sequences for demonstrating of bone marrow vertebral metastasis

Carmen Ali Zarad<sup>1\*</sup>, Ali Ahmed Abou Elmaaty<sup>2</sup> and Waleed S. Abo Shanab<sup>1</sup>

## Abstract

**Background:** This study aimed to investigate the diagnostic performance and clinical utility of different MR Dixon sequences in the characterization of vertebral metastasis in a patient with a history of malignant neoplasm and compare the results with 18-F FDG PET CT. Patients were subjected to MR imaging of the dorsal and lumbosacral spine (1.5 T MR machine) using conventional MR, T2 Dixon and T1 post-contrast Dixon.

**Results:** This study involved 40 patients (45% female and 55% male) with 161 metastatic lesions and median age 61.5 years. The sensitivities of T1 post-contrast water-only (WO), fat-only (FO) and opposed-phase (OP) Dixon for diagnosis of vertebral metastasis were 92.6%, 89.4% and 83.1%, respectively, while the sensitivity of T2 (WO, OP) Dixon was 78.3% with 100% specificity for both T1 and T2 Dixon. There were excellent positive clinical utilities of T1 post-contrast WO (0.925), FO (0.894) and OP (0.826) Dixon with the good positive clinical utility of T2 Dixon (0.783) for lesion finding. There were fair negative clinical utilities of T1 WO (0.636) and FO (0.553) Dixon with poor negative clinical utilities of T1 OP (0.429), T2 WO and OP (0.375) Dixon for lesion screening. 15% was the best in-phase/opposed-phase ratio for differentiation between metastatic and benign vertebral lesions.

**Conclusions:** MR Dixon techniques are sensitive and specific for the diagnosis of vertebral metastasis. T1 post-contrast and T2 Dixons have excellent and good positive clinical utilities for lesion finding with fair and poor negative clinical utilities for lesion screening, respectively.

**Keywords:** Vertebral metastasis, Dixon, Bone marrow, Chemical shift, Opposed phase

## Background

The spine is considered the third most common site for metastasis after lung and liver [1]. The incidence of vertebral metastases in patients with malignancy is about 10%. Vertebral metastases represent about 39% of osseous metastases [2].

Vertebral metastasis diagnosis is crucial for the selection of appropriate management of the primary tumor

and for reducing the morbidity resulting from complications or pain [2].

MRI is the most suitable imaging modality used for the detection of bone marrow lesions. T1-weighted and fat suppression fluid-sensitive sequences are the most common MRI sequences used for bone marrow metastasis detection and characterization [3, 4].

There are three types of MRI fat suppression techniques which are short tau inversion recovery sequences (STIR), chemical shift selective fat saturation pulse sequences (CHESS) and chemical shift-based water/fat separation sequences like Dixon sequence techniques [5].

Dixon [6] in 1984 joined the capabilities of MRI and spectroscopy in order to separate fat and water signals to generate water-only signal images and fat-only signal

\*Correspondence: carmenali79@yahoo.com

<sup>1</sup> Lecturer of Diagnostic Radiology, Faculty of Medicine, Port Said University, Port Fuad, Egypt

Full list of author information is available at the end of the article

images in one acquisition [7]. Dixon MR imaging technique is based on the chemical shift between water protons and fat protons [2]. Dixon technique is different than other MR fat suppression techniques because it does not permit the suppression of fat during image acquisition but permits fat suppression in the post-processing [8].

Transverse magnetization of fat and water in gradient-echo (GRE) sequence starts in-phase imaging immediately after the initial excitation pulse. These magnetizations become out-of-phase or opposition ( $180^\circ$ ) after 2.3 ms in a 1.5 T MR machine or after 1.15 ms in a 3 T MR machine. Consequently, water and fat signals are summed and creating the in-phase condition again when image acquisition has taken in TE twice the first out-of-phase condition. So with these TEs water and fat signals can be subtracted from each other [8].

By post-processing, water image is formed by summing the in-phase image, opposed-phase image and fat image (formed by subtracting the opposed-phase from the in-phase image). Measurements of fat/water fraction in a given region can be done by the Dixon technique [9].

Dixon technique can be applied with spin echo or fast spin echo sequences as well as spoiled gradient-recalled echo sequences. Dixon can be done also in T1, T2 or proton density-weighted images [10, 11]. Dixon is usually acquired in post-contrast T1 weighting sequences [12]. Four types of images are obtained by Dixon techniques, which are water-only (WO), fat-only (FO), in-phase and opposed-phase (OP) images [13, 14].

In spine MR imaging, the Dixon technique is used to obtain more homogeneous fat suppression, a larger field of view and a higher signal-to-noise ratio image with a shorter imaging time than other fat suppression MR techniques [15, 16]. Dixons are less sensitive to susceptibility artifacts than other fat suppression techniques with better detection of bony vertebral pathologies [15, 17].

This study is carried out due to the lack of knowledge in the existing literature about the diagnostic performance and clinical utility of different Dixons chemical shift MRI techniques in the characterization of vertebral metastasis.

The aim of this study is to investigate the diagnostic performance and clinical utility of different sequences of Dixon chemical shift MRI techniques in the characterization of vertebral metastasis in a patient with a history of malignant neoplasm and compare the results with fluorine 18 fluorodeoxyglucose positron emission computed tomography (18 F-FDG PET CT).

## Methods

### Patients

This study was approved by our institutional ethical committee board and was done in the period between June

2021 and December 2021. It included 40 patients with a history of primary malignant tumor and clinically suspected for vertebral metastasis.

### Inclusion criteria

- This study included all patients with a history of primary malignant tumor and highly suspected for vertebral metastasis (patient complained of constant back pain, did not relieve with bed rest and increased at night).

### Exclusion criteria

- Patients with any hematological disease with diffuse bone marrow infiltration.

## Methods

All suspected patients in the study were subjected to MR imaging of the dorsal and lumbosacral spine on a 1.5 T (Magnetom Aera, Siemens Health Care, Germany) MRI machine using a surface coil.

MRI sequences included sagittal and axial T1-weighted fast spin echo (FSE) images (540 ms repetition time (TR), 10 ms echo time (TE) and 4 mm slice thickness), sagittal and axial T2 FSE images (2850 ms repetition time (TR), 101 ms echo time (TE) and 4 mm slice thickness), and sagittal Dixon TSE T2-weighted images (3500 ms repetition time (TR), 88 ms the first echo time (TE) with automated shortest the second echo time and 4 mm slice thickness).

After that, all patients were subjected to an intravenous injection of Gd-DTPA contrast media with a dose of 0.1 mmol/kg body weight, followed by 20 ml of sterile saline solution in an antecubital vein.

Sagittal and axial post-contrast T1 Dixon images were done (400 ms repetition time (TR), 13 ms echo time (TE) and 4 mm slice thickness).

Processing and analysis of images:

All images were sent to the PACS workstation, and then sagittal T2 and sagittal post-contrast T1 Dixon chemical shift images were done. Dixon images included in-phase (IP), opposed-phase images (OP), water-only (WO = IP + OP) and fat-only (FO = IP - OP) images.

All images were evaluated in a workstation independently by two trained radiologists with more than 15 years of experience in musculoskeletal imaging.

Firstly, areas of abnormal signal intensity on the conventional T1- or T2-weighted images were compared with both T2 and post-contrast T1 Dixon chemical shift images.

The suspicious metastatic malignant lesion was detected as a homogenous low signal area compared to the skeletal muscles signal on T1 non-Dixon weighted images, low signal compared to high signal normal vertebral marrow on fat-only Dixon images, high signal compared to low signal normal vertebral marrow in T2 water-only Dixon images, high signal compared to low signal non-enhancing normal vertebral marrow in T1 post-contrast water-only Dixon images and high signal compared with low signal normal marrow in opposed-phase Dixon images.

By MRI, any vertebral lesions with intervening disk involvement were excluded from the study to exclude the possibility of false-positive results caused by spondylodiscitis. Also, any degenerative or traumatic end plate vertebral lesions were excluded.

Then, the signal intensity ratio (SIR) of the bone marrow lesions was compared on both in-phase and opposed-phase images by applying a region of interest (ROI) cursor over the abnormal area in order to quantify fat in the vertebral lesion. Three measurements were done and the average was recorded. In case of the presence of multiple lesions, the largest lesion was chosen.

The in-phase/opposed-phase ratio (IP/OP ratio) was calculated by the following equation:

$$\frac{\text{lesion signal in IP} - \text{lesion signal in OP}}{\text{lesion signal in IP}} \times 100.$$

Whole-body 18F-FDG PET CT was done for all patients after MRI as a gold standard test for the diagnosis of vertebral metastasis.

### Statistical analysis

Data were entered and analyzed using IBM-SPSS software (version 26.0). In this study, qualitative data were expressed as absolute frequency (*N*) and percentage (%). Quantitative data were initially tested for normality using Shapiro–Wilk test with data being normally distributed if  $p > 0.050$ . The presence of significant outliers was tested by inspecting boxplots. Quantitative data were expressed as median and range (minimum–maximum). Measures for assessing diagnostic test performance were calculated by Confusion Matrix Online Calculator. Clinical utility measures were calculated by Clinical Utility Index Calculator (version 4). For any of the used tests, results were considered statistically significant if  $p$  value  $\leq 0.050$ .

### Results

This study involved 40 patients [18 female (45%), and 22 male (55%)]. The patients' age ranges from 5 to 78 years with median age 61.5 years.

There were 13 types of primary tumors. The frequency of different primary tumors was 8 breast carcinoma (20%) (Fig. 1), 8 lung cancer (20%) (Figs. 2, 3), 6 prostatic carcinoma (15%), 5 colorectal carcinoma (12.5%) (Fig. 4),

1 neuroblastoma (2.5%), 2 thyroid carcinoma (5%), 1 carcinoma of the tongue (2.5%), 2 ovarian carcinoma (5%), 3 hepatocellular carcinoma (7.5%), 1 pancreatic carcinoma (2.5%), 1 nasopharyngeal carcinoma (2.5%), 1 endometrial carcinoma (2.5%) and 1 carcinoma of the urinary bladder (2.5%).

By using 18F-FDG PET scan as a gold standard test, 21 patients (52.5%) showed vertebral metastasis and 19 patients (47.5%) showed no vertebral metastasis.

In this study, 182 vertebral lesions were detected by MRI and by using 18F-FDG PET scan as a gold standard test, 161 lesions from 182 proved to be malignant (metastatic) and 21 lesions proved to be benign. There was an excellent agreement (100%) between the two readers.

Table 1 shows the diagnostic performance of T2 Dixon and T1 post-contrast Dixon images in differentiation between benign and metastatic vertebral lesion. It shows an outstanding diagnostic performance of T1 post-contrast Dixon (WO, FO and OP) and excellent diagnostic performance of T2 Dixon (WO and OP).

Table 2 shows the clinical utility of the different Dixon modalities in case finding and screening.

According to the in-phase/opposed-phase (IP/OP) ratio, there was a statically significant difference between metastatic and non-metastatic benign lesions ( $P < 0.001$ ) with a significant decrease in the in-phase/opposed-phase ratio in the metastatic lesion (ranges from 2.5 to 15%) compared with high ratio non-metastatic benign lesions (ranges from 28 to 76%) with a cut-point ratio of  $\leq 15\%$  which is a perfect discriminator of malignant lesions (Fig. 5).

### Discussion

MRI detection of metastatic vertebral lesions depends on the contrast difference between marrow-replaced metastatic lesions and normal fatty marrow [21–23]. T1-weighted images and fat suppression T2-weighted images are used widely for the diagnosis of vertebral metastasis [24, 25].

In this study, the sensitivity and specificity of T2 Dixon (WO) and (OP) were 78.3% and 100%, respectively. There were 35 false-negative vertebral lesions diagnosed by T2 Dixon (WO) and (OP). These lesions were either sclerotic vertebral metastasis that displayed low signal in all T2 Dixon sequences, small-size vertebral metastatic (less than 1cm in size) or post-treatment lesions in a patient who previously received neoadjuvant therapy [2]. These results were in agreement with the results of Hahn and his colleagues; they concluded that the sensitivity and specificity of T2 Dixon (WO) were 79.4% and 98.8%, respectively. They also reported that it was difficult to differentiate between normal



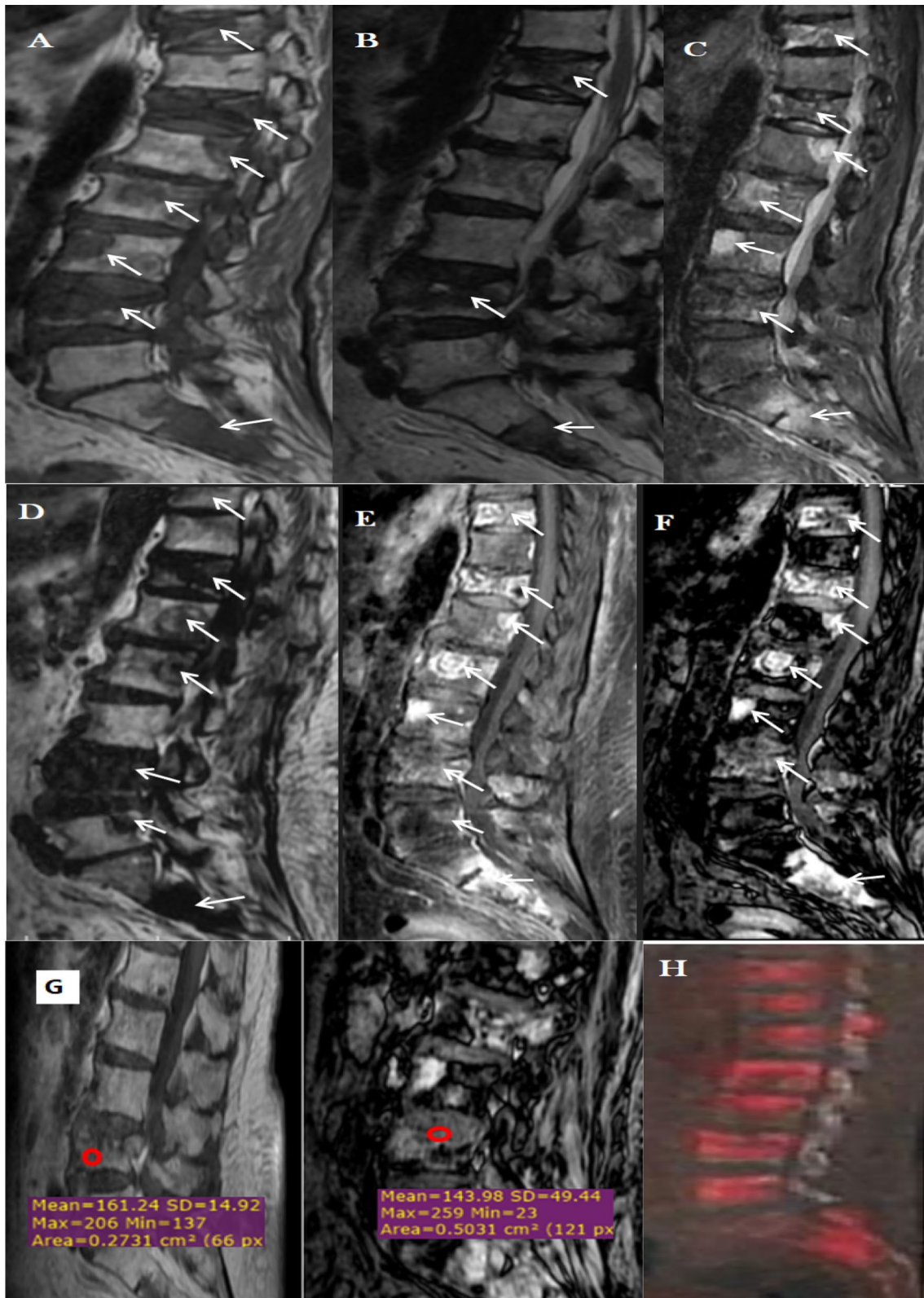


**Fig. 1** A–H MRI and PET CT images of a 64-year-old female patient with a history of breast cancer **A** T1 FSE, **B** T2 FSE, **C** T2WO Dixon, **D** T2 FO Dixon **E** T1 post-contrast WO Dixon, **F** T1 post-contrast OP Dixon, **G** IP/OP ratio MR images and **H** FDG PET CT show multiple lumbar and sacral vertebral metastasis (white arrows) with IP/OP ratio (11%)

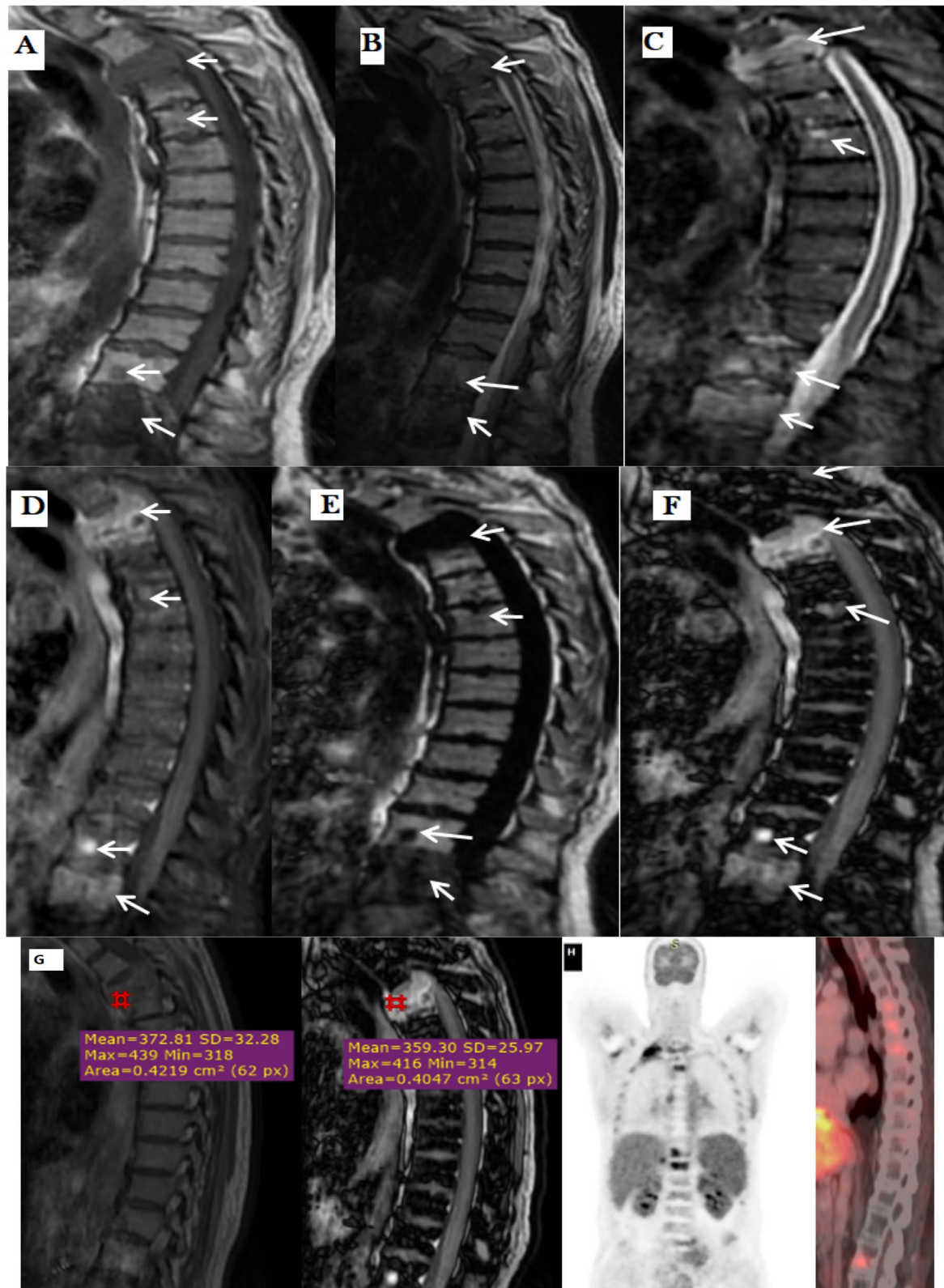


**Fig. 2** A–H MRI and PET CT images of a 56-year-old male patient with a history of lung cancer **A** T1 FSE **B** T2 FSE **C** T2 WO Dixon, **D** T1 post-contrast WO Dixon, **E** T1 FO Dixon **F** T1 post-contrast OP Dixon, **G** IP/OP ratio MR images and **H** FDG PET CT show multiple dorsal vertebral metastasis with IP/OP ratio 3.5%



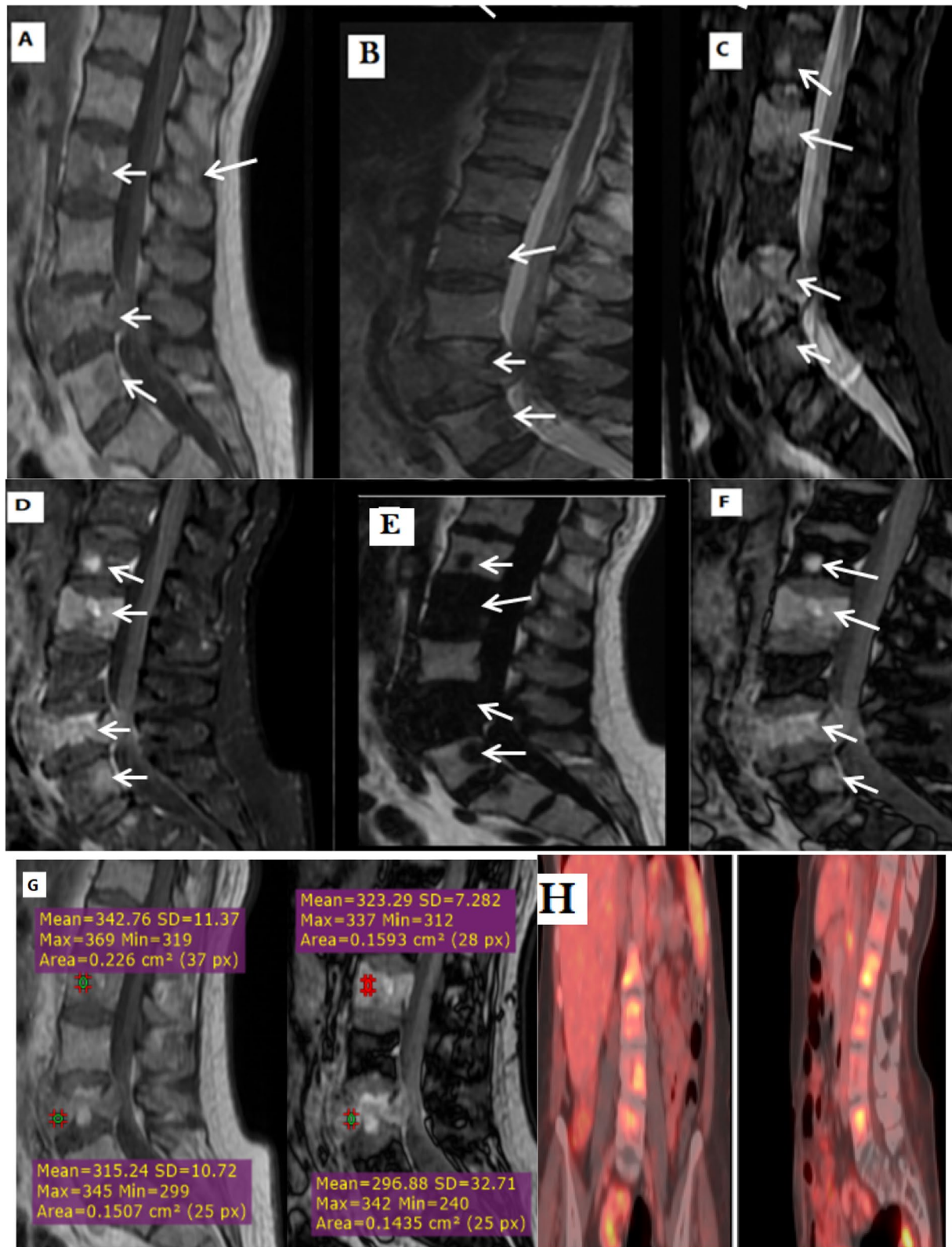


**Fig. 3** A–H MRI and PET CT images of a 69-year-old male patient with a history of lung cancer **A** T1FSE, **B** T2 FSE **C** T2 WO Dixon, **D** T1 post-contrast WO Dixon, **E** T1FO Dixon **F** T1 post-contrast OP Dixon, **G** IP/OP ratio MR images and **H** FDG PET CT show multiple lumbar vertebral metastasis (white arrows) with IP/OP ratios of two lesions (6% and 5.5%)



**Fig. 4** A–H MRI and PET CT images of a 66-year-old male patient with a history of colon cancer **A** T1 FSE, **B** T2 FSE **C** T2 WO Dixon, **D** T2 FO Dixon **E** T1 post-contrast WO Dixon, **F** T1 post-contrast OP Dixon, **G** IP/OP ratio MR images and **H** FDG PET CT show multiple dorsal vertebral metastasis (white arrows) with IP/OP ratio (9%)

**Table 1** Diagnostic performance of the T1 and T2 Dixon modalities

Measure	T2 Dixon (WO)	T2 Dixon (OP)	T1 post-contrast Dixon (WO)	T1 and T2 Dixon (FO)	T1 post-contrast Dixon (OP)
True positive	126	126	149	144	133
True negative	21	21	21	21	21
False positive	0	0	0	0	0
False negative	35	35	12	17	27
Sensitivity	78.3% (71.1%–84.4%)	78.3% (71.1%–84.4%)	92.6% (87.3%–96.1%)	89.4% (83.6%–93.7%)	83.1% (76.4%–88.6%)
Specificity	100% (83.9%–100%)	100% (83.9%–100%)	100% (83.9%–100%)	100% (83.9%–100%)	100% (83.9%–100%)
PPV	100%	100%	100%	100%	100%
NPV	37.5% (30.9%–44.6%)	37.5% (30.9%–44.6%)	63.6% (50.4%–75.1%)	55.3% (44.1%–65.9%)	43.8% (35.5%–52.3%)
LR-	21.7% (16.2%–29.1%)	21.7% (16.2%–29.1%)	7.5% (4.3%–12.8%)	10.6% (6.7%–16.6%)	16.9% (12%–23.8%)
Accuracy	80.8% (74.3%–86.2%)	80.8% (74.3%–86.2%)	93.4% (88.8%–96.5%)	90.7% (85.5%–94.5%)	85.1% (79%–89.9%)
F1 score	87.8%	87.8%	96.1%	94.4%	90.8%
MCC	54.2%	54.2%	76.7%	70.3%	60.3%
AUC	0.891 (0.837–0.933)	0.891 (0.837–0.933)	0.963 (0.924–0.985)	0.947 (0.904–0.975)	0.916 (0.865–0.952)

95% confidence intervals are presented between brackets

All measures were calculated by Confusion Matrix Online Calculator (<https://onlineconfusionmatrix.com>, accessed December 2, 2021) [18] and MedCalc Software Ltd. Diagnostic test evaluation calculator, Version 20.018 ([https://www.medcalc.org/calc/diagnostic\\_test.php](https://www.medcalc.org/calc/diagnostic_test.php), accessed December 2, 2021) [19]

PPV positive predictive value; NPV negative predictive value; LR- negative likelihood ratio; MCC Matthews correlation coefficient; AUC area under the curve

**Table 2** Clinical utility index (CUI) of the 4 modalities

Modality	+ CUI		– CUI	
	Value	Rating (for case finding)	Value	Rating (for screening)
T2 Dixon (WO) and T2 (OP)	0.783	Good	0.375	Poor
T1 post-contrast Dixon (WO)	0.925	Excellent	0.636	Fair
T1 and T2 Dixon (FO)	0.894	Excellent	0.553	Fair
T1 post-contrast (OP)	0.826	Excellent	0.429	Poor

Measures were calculated by Clinical Utility Index Calculator (version 4), <https://www.pscho-oncology.info/cui.html>, accessed December 2, 2021 [20]

CUI positive clinical utility index (sensitivity multiplied by positive predictive value); – CUI negative clinical utility index (specificity multiplied by negative predictive value)

bone marrow and adjacent osteosclerotic vertebral metastatic lesion as both lesions exhibited low signal on T2 Dixon images [2].

In the current study, the sensitivity and specificity of T1 and T2 Dixon (FO) images were the same 89.4% and 100%, respectively. Seventeen false-negative lesions were diagnosed by Dixon fat-only images. These false-negative lesions were either small vertebral metastases seen at the corner of the vertebral bodies and faulty diagnosed as Schmorl’s degenerative nodules or previously treated patients with neoadjuvant therapy. These results were matched with the results of Maeder and his colleagues they concluded that previous neoadjuvant therapy may induce the appearance of fat inside the metastatic vertebral lesions and gave false-negative

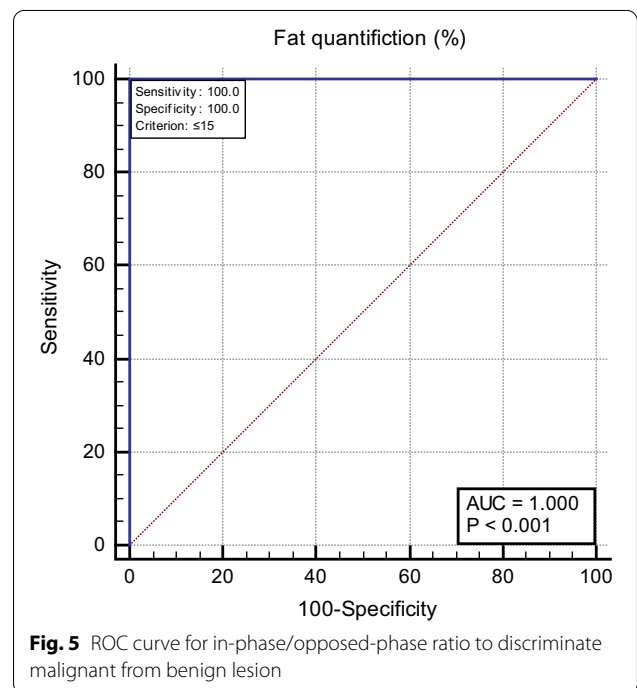


**Fig. 5** ROC curve for in-phase/opposed-phase ratio to discriminate malignant from benign lesion

results [3]. These results were also matched with the results of Zhadanov and his colleagues who reported that the ratio of T1 Dixon (FO) images for the detection of metastatic vertebral lesion was significantly higher than that of conventional T1-weighted images [26].

In the current study, the sensitivity and specificity of T1 post-contrast Dixon (OP) were 83.1% and 100%,



respectively. Twenty-seven false-negative vertebral lesions were diagnosed by T1 post-contrast Dixon (OP). These lesions were either small size vertebral metastasis (less than 1cm in size) or post-treatment vertebral lesions in previously treated patients with neoadjuvant therapy. These results were in agreement with the results of Erly and his colleagues they reported that vertebral opposed-phase imaging was sensitive and specific for differentiation between benign and malignant vertebral compression fractures.

In the current study, the sensitivity and specificity of T1 post-contrast Dixon (WO) images were 92.1% and 100%, respectively. Twelve false-negative vertebral lesions were diagnosed by T1 post-contrast (WO) Dixon. These lesions were either small size vertebral metastatic lesions less (than 1cm in size) or post-treatment vertebral lesions in previously treated patients with neoadjuvant therapy.

In this study, the sensitivity, accuracy and diagnostic performance of T1 post-contrast Dixon for detection of vertebral metastasis were higher than T2 Dixon images. As post-contrast techniques tend to increase the detection of small and osteosclerotic vertebral metastasis that cannot be detected by non-contrast T2 Dixon images. These results were in agreement with the results of Zhadanov and his colleagues they reported that T1 post-contrast Dixon images were significantly valuable for the detection of bony lesions more than non-contrast and conventional MRI techniques [26].

This study concluded that there was an outstanding diagnostic performance of T1 post-contrast Dixon (WO, FO and OP) and excellent diagnostic performances of T2 Dixon (WO and OP) in differentiation between benign and metastatic vertebral lesions. These results were in agreement with the results of Hahn and his colleagues they demonstrated excellent diagnostic performance of T1 and T2 Dixon in the detection of vertebral metastasis [2].

As regards the clinical utility of different Dixon modalities in the finding of vertebral metastasis, this study concluded that there were excellent positive clinical utility of T1 post-contrast Dixon (WO, FO and OP) and good positive clinical utility of T2 Dixon (WO and OP).

Regarding the clinical utility of different Dixon modalities in the screening of vertebral metastasis, the current study concluded that there were fair negative clinical utility of T1 post-contrast Dixon (WO and FO) and poor negative clinical utility of T2 Dixon (WO and OP).

Dixon chemical shift imaging added potential values in challenging examinations with common pitfalls that can be encountered when dealing with spine MR imaging. Dixon could be used to identify typical vertebral hemangiomas as it usually shows a significantly decreased signal on the OP images compared with the increased signal

of malignant vertebral lesions. Dixon showed promising results in differentiation between malignant and osteoporotic vertebral fractures, as in osteoporotic vertebral fractures fatty marrow remains, while in malignant vertebral fracture fatty marrow is replaced by malignant tissues. Dixon can differentiate between vertebral metastases and degenerative bone marrow changes [27].

Many studies reported that the comparison of metastatic lesion signal intensity between in-phase and opposed-phase Dixon images was valuable for the diagnosis of vertebral metastasis [13, 23, 28, 29].

In this study, as regard the in-phase/opposed-phase (IP/OP) ratio there was a statically significant difference between metastatic and non-metastatic benign lesions ratios ( $P < 0.001$ ) with a significant decrease in ratio in metastatic lesion compared with a high ratio of non-metastatic benign lesions. These results were in agreement with the results of the study of Donners and his colleagues who reported that the ratio of fat fraction was significantly lower in malignant vertebral fractures compared to osteoporotic fractures [30].

By using the ROC curve analysis, the current study concluded that 15 % was the best IP/OP ratio cut-point value for differentiation between malignant and benign lesions with 100 % sensitivity, 100% specificity and 100% diagnostic accuracy. In contrast, the study of Pozzi and his colleagues concluded that the use of apparent diffusion coefficient (ADC) cutoff value showed a significant overlap between benign and malignant lesions with 81.3% sensitivity, 55% specificity and 76% diagnostic accuracy [31].

In the current study, the IP/OP ratio cut-point value was slightly higher than that calculated by the study of Donners and his colleagues as they concluded that the best cutoff value for differentiation between malignant and benign lesion was 11.5 % and this may be due to the use of different formula for calculation of the ratio between the two studies [30].

The ongoing introduction of artificial intelligence allows new imaging tools and applications. The study of Gitto and colleagues reported that a support vector machine (SVM) model that depends on T2-weighted images and ADC maps radiomic features can differentiate between benign and malignant vertebral lesions with 76% accuracy [32].

## Conclusions

MR Dixon techniques are sensitive and specific for the diagnosis of vertebral metastasis. T1 post-contrast and T2 Dixons have excellent and good positive clinical utilities for lesion finding with fair and poor negative clinical utilities for lesion screening, respectively.

### Abbreviations

STIR: Short tau inversion recovery; CHESS: Chemical shift selective fat saturation pulse sequences; GRE: Gradient echo; TEs: Echo times; SE: Spin echo; 18 F-FDG PET CT: Fluorine 18 fluorodeoxyglucose positron emission computed tomography; IP: In-phase; OP: Opposed phase; WO: Water only; FO: Fat only; SIR: Signal intensity ratio; ROI: Region of interest; IP/OP ratio: In-phase/opposed-phase ratio; ADC: Apparent diffusion coefficient; SVM: Support vector machine.

### Acknowledgements

Not applicable.

### Author contributions

CAZ, AAA and WSA carried out the work. CAZ and AAA designed the study, CAZ, AAA and WSA collected the patients and gathered the data. CAZ and WSA collected and reported the radiological data. CAZ and AAA did the statistical analysis and were responsible for collecting the scientific data and writing the manuscript. All authors read and approved the final version to be published.

### Funding

Not applicable.

### Availability of data and materials

All data and material of the article are readily available.

### Declarations

#### Ethics approval and consent to participate

The authors obtained permission to conduct this study which was approved by Research Ethic Committee (REC) at the Faculty of Medicine, Port Said University, Port Said, Egypt (Serial.no [18] RAD\_003), and all participants gave written informed consent. The procedures followed were in accordance with our protocol.

#### Consent for publication

All participants gave written informed consent.

#### Competing interests

The authors declare that they have no competing interests.

#### Author details

<sup>1</sup>Lecturer of Diagnostic Radiology, Faculty of Medicine, Port Said University, Port Fuad, Egypt. <sup>2</sup>Lecturer of Neurology, Faculty of Medicine Helwan University, Helwan, Egypt.

Received: 7 January 2022 Accepted: 1 August 2022

Published online: 09 August 2022

### References

- Lubdhra MS, Karen LS (2011) Imaging of spinal metastatic disease. *Int J Surg Oncol Vol* 769753:12
- Hahn S, Lee YH, Suh JH (2018) Detection of vertebral metastases: a comparison between the modified Dixon turbo spin echo T2 weighted MRI and conventional T1 weighted MRI: a preliminary study in a tertiary centre. *Br J Radiol* 91:20170782
- Maeder Y, Dunet V, Richard R, Becce F, Omoumi P (2018) Bone Marrow metastases: T2-Weighted Dixon spin-echo fat images can replace T1-weighted spin-echo images. *Radiology* 286(3):948–959
- Hong SH, Choi JY, Lee JW, Kim NR, Choi JA, Kang HS (2009) MR imaging assessment of the spine: infection or an imitation? *Radiographics* 29:599–612
- Pezeshk P, Alian A, Chhabra A (2017) Role of chemical shift and Dixon based techniques in musculoskeletal MR imaging. *Eur J Radiol* 94:93–100. <https://doi.org/10.1016/j.ejrad.2017.06.011>
- Dixon WT (1984) Simple proton spectroscopic imaging. *Radiology* 153:189–194
- Özgen A (2017) The value of the T2-weighted multipoint Dixon sequence in MRI of sacroiliac joints for the diagnosis of active and chronic sacroiliitis. *AJR Am J Roentgenol* 208:603–608
- Grimm A, Meyer H, Nickel MD et al (2018) Evaluation of 2-point, 3-point, and 6-point Dixon magnetic resonance imaging with flexible echo timing for muscle fat quantification. *Eur J Radiol* 103:57–64
- Yoo HJ, Hong SH, Kim DH et al (2017) Measurement of fat content in vertebral marrow using a modified dixon sequence to differentiate benign from malignant processes. *J Magn Reson Imaging* 45(1534–44):16
- Burakiewicz J, Sinclair CDJ, Fischer D et al (2017) Quantifying fat replacement of muscle by quantitative MRI in muscular dystrophy. *J Neurol* 264:2053–2067
- Park EH, Lee KB (2017) Usefulness of black boundary artifact on opposed-phase imaging from turbo spin-echo two-point mDixon M for delineation of an arthroscopically confirmed small fracture of the lateral talar dome: a case report. *Medicine (Baltimore)* 96:e9497
- Pezeshk P, Alian A, Chhabra A (2017) Role of chemical shift and Dixon based techniques in musculoskeletal MR imaging. *Eur J Radiol* 94:93–100
- Douis H, Davies AM, Jeys L, Sian P (2016) Chemical shift MRI can aid in the diagnosis of indeterminate skeletal lesions of the spine. *Eur Radiol* 26:932–940
- Lins CF, Salmon CEG, Nogueira-Barbosa MH (2021) Applications of the Dixon technique in the evaluation of the musculoskeletal system. *Radiol Bras* 54(1):33–42
- Guerini H, Omoumi P, Guichoux F et al (2015) Fat suppression with Dixon techniques in musculoskeletal magnetic resonance imaging: a pictorial review. *Semin Musculoskelet Radiol* 19:335–347
- Kirchgesner T, Perlepe V, Michoux N, Larbi A, Vande Berg B (2017) Fat suppression at 2D MR imaging of the hands: Dixon method versus CHESS technique and STIR sequence. *Eur J Radiol* 89:40–46
- Low RN, Austin MJ, Ma J (2011) Fast spin-echo triple echo dixon: Initial clinical experience with a novel pulse sequence for simultaneous fat-suppressed and nonfat-suppressed T2-weighted spine magnetic resonance imaging. *J Magn Reson Imaging* 33(2):390–400
- Confusion Matrix Online Calculator (<https://onlineconfusionmatrix.com>)
- Diagnostic test evaluation calculator, Version 20.018 ([https://www.medcalc.org/calc/diagnostic\\_test.php](https://www.medcalc.org/calc/diagnostic_test.php))
- Clinical Utility Index Calculator (version 4), <https://www.psyo-oncology.info/cui.html>
- Bollen L, Dijkstra SPD, Bartels RHMA, de Graeff A, Poelma DLH, Brouwer T et al (2018) Clinical management of spinal metastases-the dutch national guideline. *Eur J Cancer* 104:81–90
- Howe BM, Johnson GB, Wenger DE (2013) Current concepts in MRI of focal and diffuse malignancy of bone marrow. *Semin Musculoskelet Radio* 17(2):137–144
- Shah LM, Hanrahan CJ (2011) MRI of spinal bone marrow: part I, techniques and normal age-related appearances. *AJR Am J Roentgenol* 197:1298–1308
- Del Grande F, Subhawong T, Flammang A, Fayad LM (2014) Chemical shift imaging at 3 Tesla: effect of echo time on assessing bone marrow abnormalities. *Skeletal Radiol* 43:1139–1147
- Lecouvet FE (2016) Whole-body MR imaging: musculoskeletal applications. *Radiology* 279(2):345–365
- Zhadanov SI, Doshi AH, Pawha PS, Corcuera-Solano I, Tanenbaum LN (2016) Contrast-enhanced Dixon fat-water separation imaging of the spine: added value of fat, in-phase and opposed-phase imaging in marrow lesion detection. *J Comput Assist Tomogr* 40(6):985–990
- Albano D, Messina C, Gitto S, Papakonstantinou O, Sconfienza LM (2019) Differential diagnosis of spine tumor my favorite mistake. *Semin Musculoskelet Radiol* 23:26–35
- Ragab Y, Emad Y, Gheita T et al (2009) Differentiation of osteoporotic and neoplastic vertebral fractures by chemical shift in-phase and out-of-phase MR imaging. *Eur J Radiol* 72(1):125–133
- Zajick DC Jr, Morrison WB, Schweitzer ME, Paredada JA, Carrino JA (2009) Benign and malignant processes: normal values and differentiation with chemical shift MR imaging in vertebral marrow. *Radiology* 237(2):590–596
- Donners R, Obmann MM, Boll D, Gutzeit A, Harder D (2020) Dixon or DWI – comparing the utility of fat fraction and apparent diffusion coefficient to distinguish between malignant and acute osteoporotic vertebral fractures. *Eur J Radiol* 132:109342

31. Pozzi G, Albano D, Messina C, Alessio Angileri S, Al-Mnayyis A, Galbusera F et al (2018) Solid bone tumors of the spine: diagnostic performance of apparent diffusion coefficient measured using diffusion-weighted MRI using histology as a reference standard. *J Magn Reson Imaging* 47:1034–1042
32. Gitto S, Bologn M, Corino VDA, Emili I, Albano D, Messina C et al (2022) Diffusion weighted MRI radiomics of spine bone tumors: feature stability and machine learning based classification performance. *Radiol Med (Torino)* 127:518–525

### **Publisher's Note**

Springer Nature remains neutral with regard to jurisdictional claims in published maps and institutional affiliations.

**Submit your manuscript to a SpringerOpen<sup>®</sup> journal and benefit from:**

- ▶ Convenient online submission
- ▶ Rigorous peer review
- ▶ Open access: articles freely available online
- ▶ High visibility within the field
- ▶ Retaining the copyright to your article

---

Submit your next manuscript at ▶ [springeropen.com](https://www.springeropen.com)

---